Electronic Supplementary Material (ESI) for Dalton Transactions.

Supporting Information

Fluorescent BF_2 Complexes of Pyridyl-isoindoline-1-ones: Synthesis, Characterization and Their Distinct Response to Mechanical Force

Meifang Liu[a,*], Yi Han[b], Wei Yuan[b], Changxiang Guo[b], Shiling Shi[b], Xia Liu[b] and Yulan Chen[b,*]

[a] College of Chemistry-Chemical & Environmental Engineering, Weifang University, Weifang, 261061, P. R. China

E-mail: liumf@iccas.ac.cn (M. Liu)

Phone/Fax: +86-536-8785283

[b] Institute of Molecular Plus, Tianjin University, Tianjin, 300072, P. R. China

E-mail: yulan.chen@tju.edu.cn (Y. Chen);

1. **Materials and instruments**

All reagents were purchased from Acros or Aldrich and used without further purification. Tetrahydrofuran was dried with sodium and benzophenone. Dichloromethane was dried with CaH_2. Others reagents and solvents were dealt with standard procedure. $Pd(PPh_3)_4$ was synthesized according to the reference [*S1*], and charged with nitrogen in a Schlenk tube.

The UV-vis absorption spectra were recorded on a PerkinElmer Lambda 750 spectrophotometer. Fluorescence spectra and quantum yields of solid powders were recorded on a Hitachi F-7000 fluorescence spectrophotometer. The transient fluorescence decay curves were measured on an Edinburgh FLS 920 fluorescence spectrometer. Mass spectra were obtained with a matrix-assisted laser desorption ionization time-of-flight (MALDI-TOF) mass spectrometer. ^{13}C NMR, ^{11}B NMR, ^{19}F NMR and ^{1}H NMR spectra were recorded on a Bruker instrument at 400 MHz by using solvent: DMSO-d_6 or $CDCl_3$. Thermogravimetric analyses (TGA) were carried out using a TA Instruments Q-50 with a heating rate of 10 ^{o}C/min. DSC measurements were recorded using the TA Instruments Q-20 with a scan rate of 10 ^{o}C/min. The powder XRD patterns were obtained with a Rigaku Smart Lab (9 kW) X-ray diffractometer. Single crystals were obtained in the mixture of acetate, hexane and CH_2Cl_2 for **B2** by a slow solvent diffusion method. The single crystal X-ray diffraction was carried out on a Rigaku SCX-mini diffractometer with graphite monochromatic Mo-Kα radiation (λ=0.7173Å) by ω scan mode. Density functional theory (DFT) calculations were performed in Gaussian 09 software at the B3LYP functional with the 6-31G* basis set level.

2. **Synthesis**

B1 was synthesized according to the reference [*S2*]. ^{1}H NMR (400 MHz, $CDCl_3$, ppm) δ 8.72 (d, *J* = 6.0 Hz, 1H), 8.11-7.88 (m, 2H), 7.80-7.70 (m, 1H), 7.61 (pd, *J* = 7.4, 1.3 Hz, 2H), 7.52-7.37 (m, 2H),

6.32 (s, 1H). ^{11}B NMR (128 MHz, $CDCl_3$, ppm) δ1.98 (s), 1.75 (s), 1.52 (s). ^{19}F NMR (376 MHz, $CDCl_3$, ppm) δ -138.72, -138.80, -138.88, -138.95.

4 and **5** were synthesized according to the references [*S3*,*S4*]

*2.1 Synthesis of Compound **1**.*

1 was synthesized according to the reference [*S2*]. Isoindolin-1-one (0.40 g, 3 mmol), 5-bromopyridine- 2-carbaldehyde (1.02 g, 6 mmol), and K_2CO_3 (0.80 g, 6 mmol), the yield of **1** (0.44 g, 48%). ^{1}H NMR (400 MHz, $CDCl_3$, ppm) δ 8.63 (d, *J* = 2.3 Hz, 1H), 7.93-7.85 (m, 1H), 7.83-7.72 (m, 2H), 7.63 (td, *J* = 7.5, 1.1 Hz, 1H), 7.55 (td, *J* = 7.4, 0.9 Hz, 1H), 7.18 (d, *J* = 8.4 Hz, 1H), 6.30 (s, 1H). ^{13}C NMR (100 MHz, $CDCl_3$, ppm) δ 168.61, 154.12, 150.16, 139.33, 138.61, 137.68, 132.19, 129.99, 129.40, 125.24, 123.79, 120.11, 117.57, 100.67, 100.00. MALDI-TOF (m/z), calculated: $C_{14}H_9BrN_2O$ $[M+H]^+$ 300.99; found: 301.00

*2.2 Synthesis of Compound **2**.*

A mixture of **1** (0.2 g, 1.5 mmol), **4** (0.7g, 1.5 mmol), K_2CO_3 (0.6g, 4.5 mmol), THF (15 mL) and H_2O (5 mL) and $Pd(PPh_3)_4$ (35 mg, 0.03 mmol) was charged with nitrogen. The reaction mixture was stirred and refluxed for overnight. CH_2Cl_2 was added, then the mixture was dried with Na_2SO_4. The residue was chromatographically purified on silica gel eluting with PE/CH_2Cl_2 (5:1, v:v) to afford **2** as an orange solid (0.55 g, 67%). ^{1}H NMR (400 MHz, $CDCl_3$, ppm) δ 8.83 (s, 1H), 8.10 (d, *J* = 8.5 Hz, 1H), 7.93 (d, *J* =7.3 Hz, 1H), 7.73 (d, *J* = 7.1 Hz, 1H), 7.59 (dt, *J* = 14.7, 7.3 Hz, 2H), 7.47 (d, *J* = 8.5 Hz, 1H), 7.36 (d, *J* = 8.0 Hz, 2H), 7.21-7.10 (m, 11H), 7.10-7.00 (m, 6H), 6.33 (s, 1H). ^{13}C NMR (100 MHz, $CDCl_3$, ppm) δ 168.71, 154.26, 147.43, 143.90, 143.59, 143.55, 141.64, 140.19, 138.00, 137.87, 134.99, 134.49, 133.29, 132.21, 132.03, 131.41, 131.37, 131.34, 129.73, 129.53, 127.88, 127.82, 127.70, 126.70, 126.64, 126.58, 125.97, 124.21, 123.74, 120.05, 101.72. MALDI-TOF (m/z),

calculated: $C_{40}H_{28}N_2O$ $[M+H]^+$ 553.22; found: 553.18.

*2.3 Synthesis of Compound **3**.*

The synthetic method of **3** is similar to that of **2**.

1 (0.2 g, 1.5 mmol), **5** (0.67 g, 1.8 mmol), K_2CO_3 (0.6 g, 4.5 mmol), THF (15 mL) and H_2O (5 mL), $Pd(PPh_3)_4$ (35 mg, 0.03 mmol), **3** as an orange solid (0.54 g, 78%). ^{1}H NMR (400 MHz, $CDCl_3$, ppm) δ 11.24 (s, 1H), 8.82 (d, *J* = 2.2 Hz, 1H), 7.84 (ddd, *J* = 26.8, 22.4, 7.5 Hz, 3H), 7.63 (t, *J* = 7.5 Hz, 1H), 7.57-7.46 (m, 3H), 7.31 (dd, *J* = 17.0, 8.6 Hz, 6H), 7.20-7.13 (m, 5H), 7.07 (t, *J* = 7.3 Hz, 2H), 6.40 (s, 1H). ^{13}C NMR (100 MHz, $CDCl_3$, ppm) δ 168.72, 153.82, 148.14, 147.38, 147.18, 137.90, 137.81, 134.11, 133.38, 132.01, 130.61, 129.67, 129.53, 129.43, 127.52, 124.83, 124.29, 123.75, 123.46, 123.44, 120.03, 101.81. MALDI-TOF (m/z), calculated: $C_{32}H_{23}N_3O$ $[M]^+$ 465.18; found: 465.15.

2.4 Synthesis of Compound **B2 and B3**.

At 0 °C, triethylamine was added to **2** or **3** in dry CH_2Cl_2. $BF_3{\cdot}Et_2O$ was added dropwise. The reaction mixture was stirred overnight at 25°C. The reaction was quenched by adding water (10 mL) and the mixture was extracted with CH_2Cl_2 (3 × 50 mL). The organic phase was dried by anhydrous Na_2SO_4. The residue was purified chromatographically on Al_2O_3 gel eluting with PE/EtOAC (5:1, v:v).

B2: 2 (1.10 g, 2 mmol), CH_2Cl_2 (60 mL), triethylamine (4 mL, 28 mmol) and $BF_3{\cdot}Et_2O$ (4 mL, 30 mmol) were used to afford **B2** as a red powder (1.07 g, 89%).

^{1}H NMR (400 MHz, $CDCl_3$, ppm) δ 8.83 (s, 1H), 8.10 (d, *J* = 8.5 Hz, 1H), 7.93 (d, *J* = 7.3 Hz, 1H), 7.73 (d, *J* = 7.1 Hz, 1H), 7.59 (dt, *J* = 14.7, 7.3 Hz, 2H), 7.47 (d, *J* = 8.5 Hz, 1H), 7.36 (d, *J* = 8.0 Hz, 2H), 7.26 (s, 2H), 7.24 - 6.93 (m, 13H), 6.33 (s, 1H), 5.30 (s, 1H). ^{13}C NMR (100 MHz, $CDCl_3$, ppm) δ 171.23, 148.41, 146.40, 145.40, 143.34, 143.32, 143.22, 142.28, 140.28, 139.71, 139.53, 136.10, 134.68,

132.55, 132.42, 132.16,131.42, 131.34, 131.32, 131.28, 131.18, 127.98, 127.91, 127.74, 126.94, 126.79, 126.74, 125.90, 124.25, 121.02, 92.89. MALDI-TOF (m/z), calculated: $C_{40}H_{27}BF_2N_2O$ $[M]^+$ 600.22; found: 600.12. ^{11}B NMR (128 MHz, $CDCl_3$, ppm) δ 1.80 (s). ^{19}F NMR (376 MHz, $CDCl_3$, ppm) δ -138.84.

B3: 3 (0.93 g, 2 mmol), CH_2Cl_2 (60 mL), triethylamine (4 mL, 28 mmol) and $BF_3{\cdot}Et_2O$ (4 mL, 30 mmol) were used to afford **B3** as a red powder (0.94 g, 92%). ^1H NMR (400 MHz, $CDCl_3$, ppm) δ 8.86 (s, 1 H), 8.12 (dd, *J* = 8.5, 1.9 Hz, 1 H), 7.94 (d, *J* = 6.8 Hz, 1 H), 7.74 (d, J =7.1 Hz, 1 H), 7.65 – 7.55 (m, 2 H), 7.47 (t, *J* = 8.5 Hz, 3 H), 7.32 (t, *J* = 7.8 Hz, 4 H), 7.20 – 7.06 (m, 8 H), 6.33 (s, 1 H). ^{13}C NMR (100 MHz, $CDCl_3$, ppm) δ 149.32, 147.86, 146.97, 139.87, 139.08, 136.21, 134.83, 132.35, 131.33, 129.56, 127.41, 127.10, 125.27, 124.31, 124.02, 122.70, 120.93, 92.90. MALDI-TOF (m/z), calculated: $C_{32}H_{22}BF_2N_3O$ $[M]^+$ 513.18; found: 513.12. ^{11}B NMR (128 MHz, $CDCl_3$, ppm) δ 1.83 (s). ^{19}F NMR (376 MHz, $CDCl_3$, ppm) δ -139.11.

3. Photophysical properties in solution

Table S1. Photophysical properties of **B1**, **B2** and **B3**

	B1					B2					B3				
	$^{a}\lambda_{abs}$ (nm)	$^{b}\lambda_{em}$ (nm)	$^{c}\nu$ (nm)	$^{d}\Delta\lambda$ (nm)	$^{e}\varepsilon$ ($LM^{-1}cm^{-1}$)	$^{a}\lambda_{abs}$ (nm)	$^{b}\lambda_{em}$ (nm)	$^{c}\nu$ (nm)	$^{d}\Delta\lambda$ (nm)	$^{e}\varepsilon$ ($LM^{-1}cm^{-1}$)	$^{a}\lambda_{abs}$ (nm)	$^{b}\lambda_{em}$ (nm)	$^{c}\nu$ (nm)	$^{d}\Delta\lambda$ (nm)	$^{e}\varepsilon$ ($LM^{-1}cm^{-1}$)
toluene	400	462	62	~	$2.8x10^{4}$	427	499	72	~	$3.8x10^{4}$	450	536	86	~	$2.9x10^{4}$
chloroform	395	455	60	~	$2.8x10^{4}$	425	557	132	~	$4.0x10^{4}$	455	610	155	~	$2.9x10^{4}$
THF	396	455	59	~	$2.6x10^{4}$	422	530	108	~	$4.2x10^{4}$	443	613	170	~	$3.1x10^{4}$
DMF	394	455	61	~	$2.9x10^{4}$	422	weak	~	~	$3.8x10^{4}$	446	n.d.	~	~	$3.1x10^{4}$
CH_3CN	390	452	62	~	$2.8x10^{4}$	416	weak	~	~	$3.6x10^{4}$	440	n.d.	~	~	$3.2x10^{4}$
pristine		472		5			537		35			600		50	
ground		477					572					650			

^{a}Maximum absorption; ^{b}Maximum emission; ^{c}Stokes shift; ^{d}Red shift value of fluorescence maximum after ground; ^{e}Absorption coefficient in chloroform at the maximum absorption wavelength.

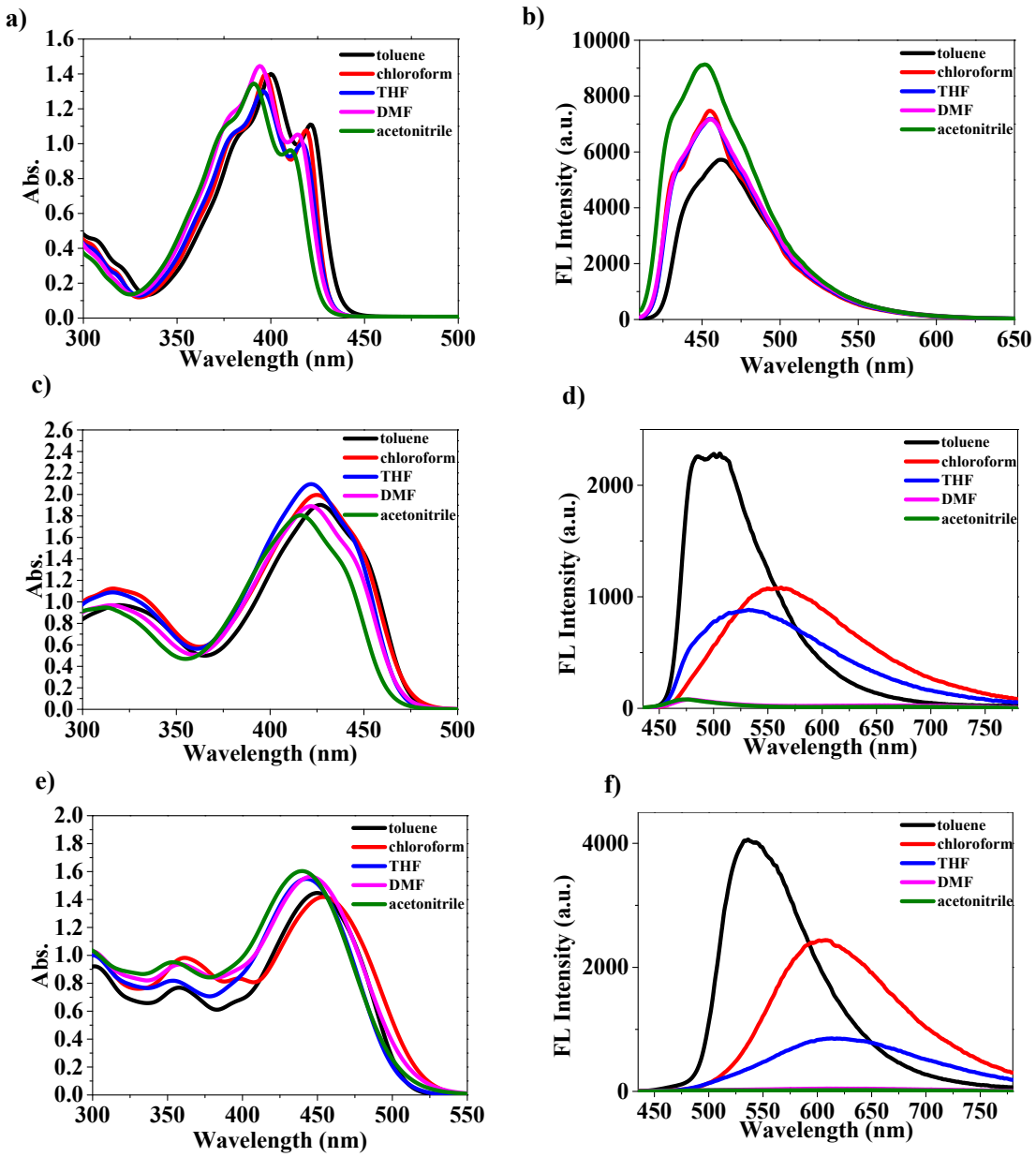

Figure S1. UV-vis absorption spectra of (a) **B1**, (c) **B2** and (e) **B3** (5×10^{-5} M) in various solvents; fluorescence spectra of (b) **B1**, (d) **B2** and (f) **B3** (5×10^{-5} M, excited at 410 nm for **B1**, excited at 425nm for **B2** and **B3**) in various solvents.

4. **Photophysical properties in solid states**

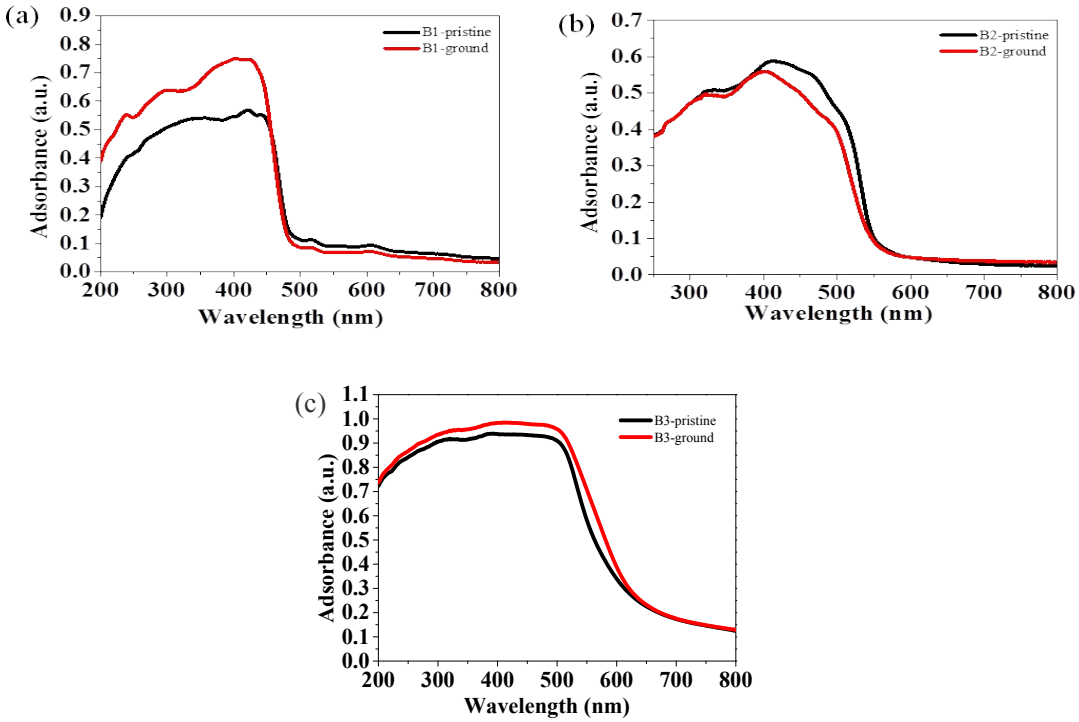

Figure S2. UV-vis spectra of (a) **B1**, (b) **B2** and (c) **B3** in different solid states.

Table S2. The fluorescence quantum yields (Φ_F) of **B1**, **B2** and **B3** in solid state

compound	$\Phi_{F\ pristine}$ (%)[a]	$\Phi_{F\ ground}$ (%)[a]
B1	12.2	7.2
B2	8.6	8.6
B3	1.9	1.8

[a] The fluorescence quantum yields were measured with an absolute fluorescence quantum yield spectrometer.

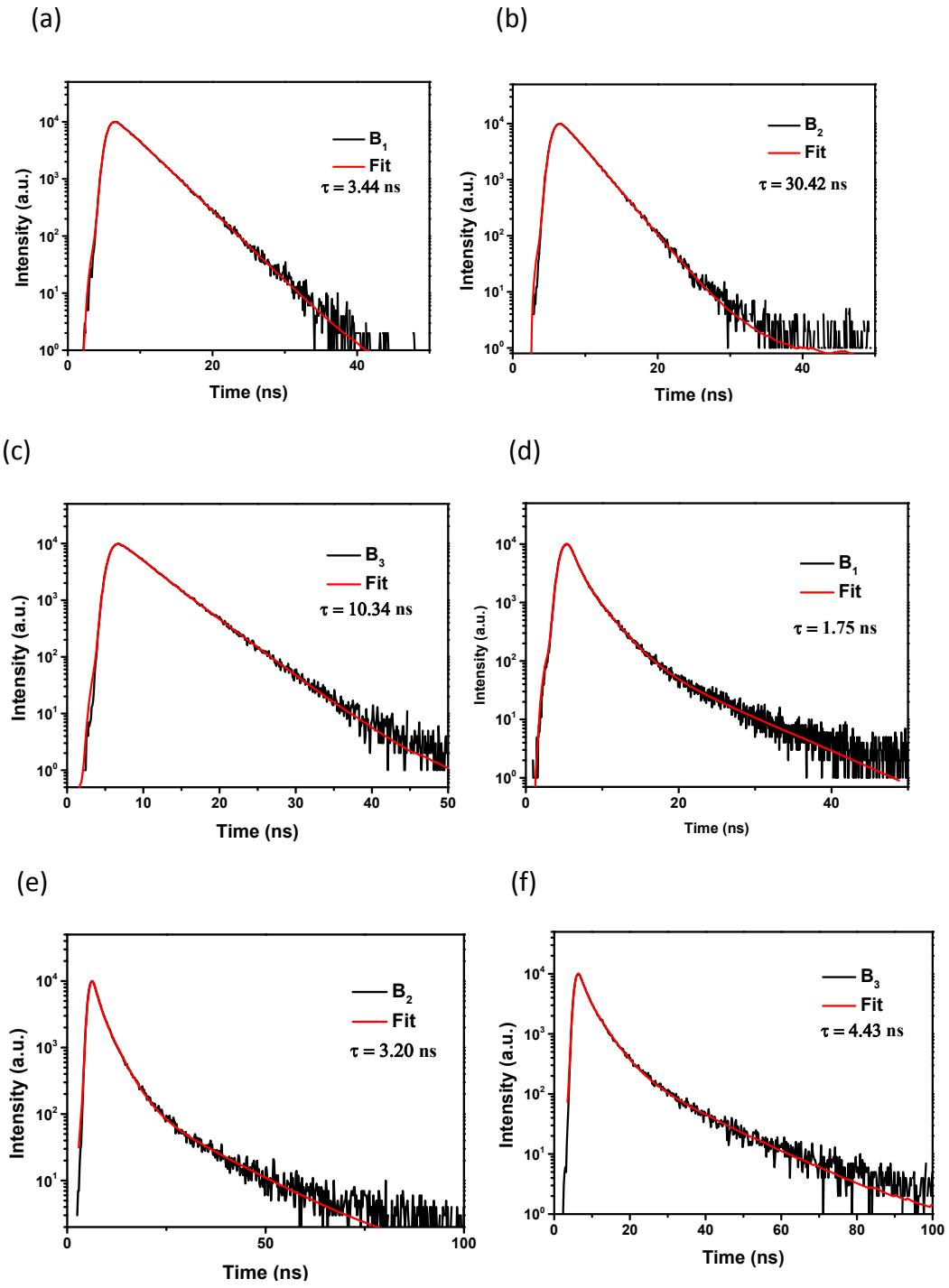

Figure S3. Fluorescence decay curve (black line) of (a) **B1**, (b) **B2**, (c) **B3** in solution (CH_2Cl_2); (d) **B1**, (e) **B2**, (f) **B3** in film.

Table S3. Optical parameters of **B1**, **B2** and **B3**

	fluorescence lifetime (ns)		Φ_F (%)
	In solution	In solid state	
B1	3.44	1.75	65.5
B2	30.42	3.20	19.3
B3	10.34	4.43	10.0

Φ_F: The fluorescence quantum yields were determined by a relative method for solution with 3-(2-benzothiazolyl)-N,N-diethylumbelliferylamine (in CH_2Cl_2, Φ_F = 76%) as a standard.

5. **Density functional theory (DFT) calculations**

Table S4. Calculated dipole moments for **B1**, **B2** and **B3**

Compound	**B1**	**B2**	**B3**
Dipole Moment (Debye)	7.9282	7.9306	8.1819

1.

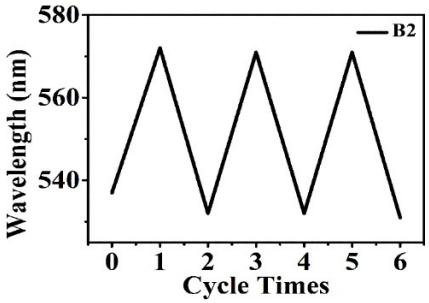

Figure S4. Reversible switching of fluorescence emission of **B2** by repeated grinding/fuming cycles.

2. Single crystal structures and data

Table S5. Crystal data of **B2** (CCDC:1888230)

Experical formula	**$C_{40}H_{27}BF_2N_2O$**
Space group	**P-1**
Cell lengths	**a/Å 10.517(2) b/Å 11.328(2) c/Å 15.112(3)**
Cell angles	**α/° 88.40(3) β/° 84.21(3) γ/° 77.10(3)**
Cell volume	**1745.97/Å^3**
Z, Z'	**Z: 2, Z': 0**
R-Factor (%)	**5.61**

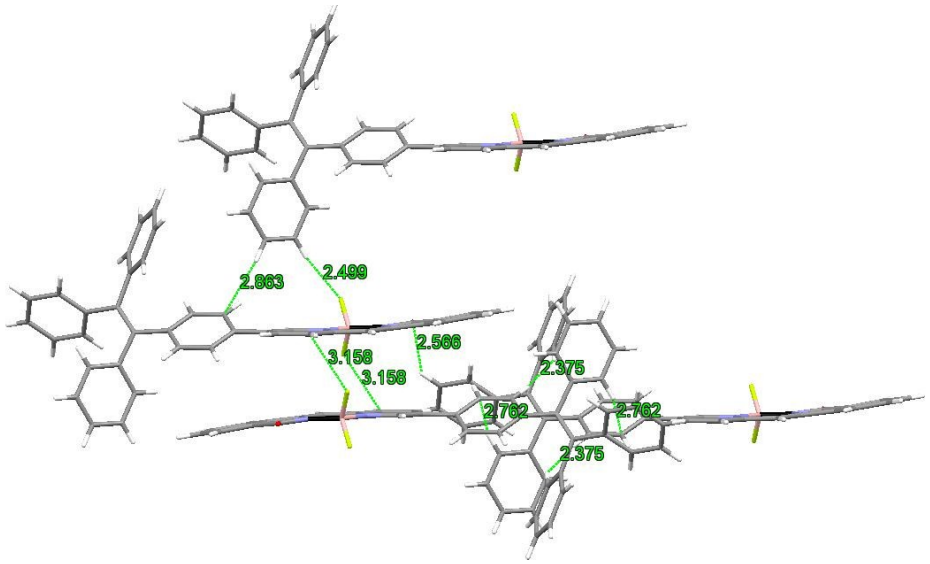

Figure S5. Multiple intermolecular interactions existed in the crystals, including B-F···H–C, F-B···C and C=O···H-C interactions.

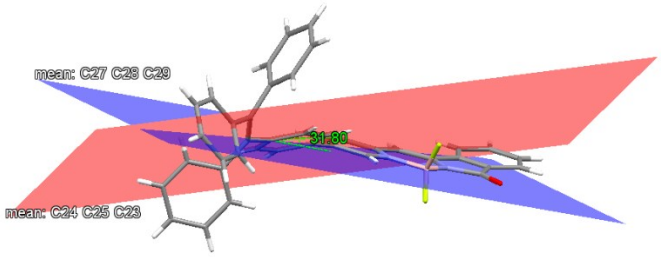

Figure S6. Dihedral angle of **B2**.

3. **TGA curves**

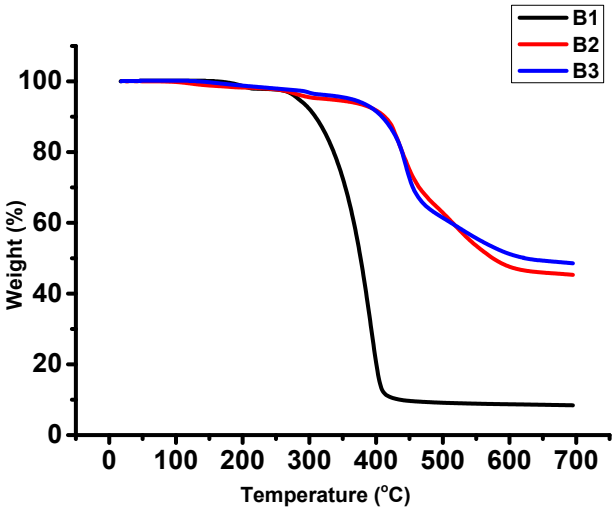

Figure S7. TGA curves of (a) **B1**, (b) **B2** (c) **B3** pristine samples. The decomposition temperature is about 283 °C for **B1**, 326 °C **B2** for and 363 °C for **B3**.

4. **DSC curves**

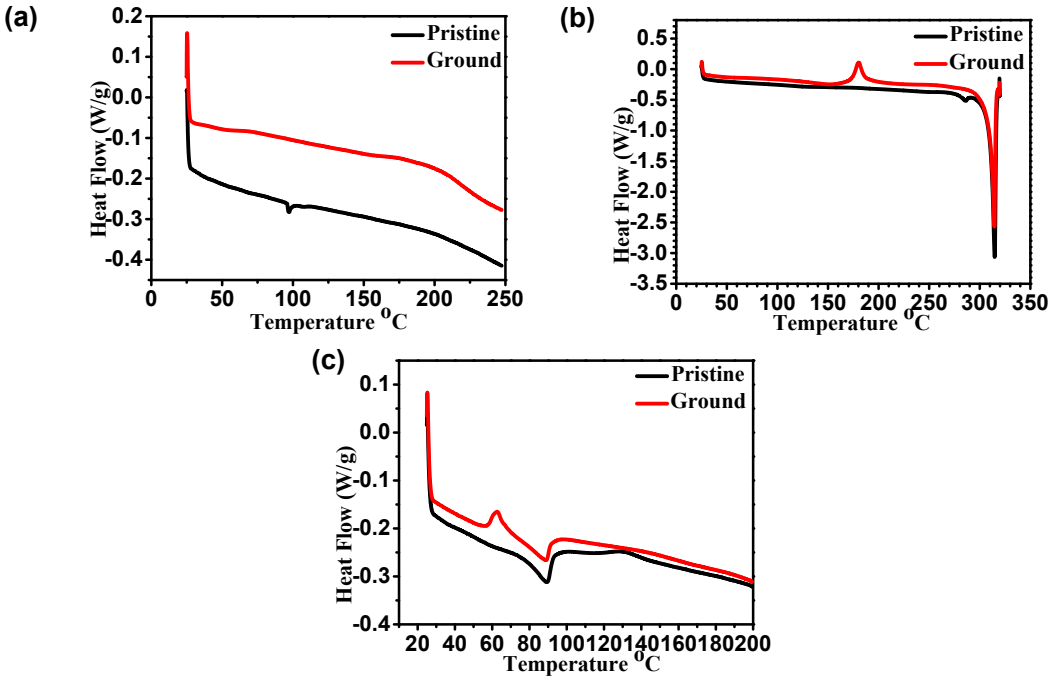

Figure S8. DSC curves for the pristine and ground samples of (a) **B1**, (b) **B2**, (c) **B3** (scan rate: 10 °C min^{-1}).

5. **NMR and mass spectra**

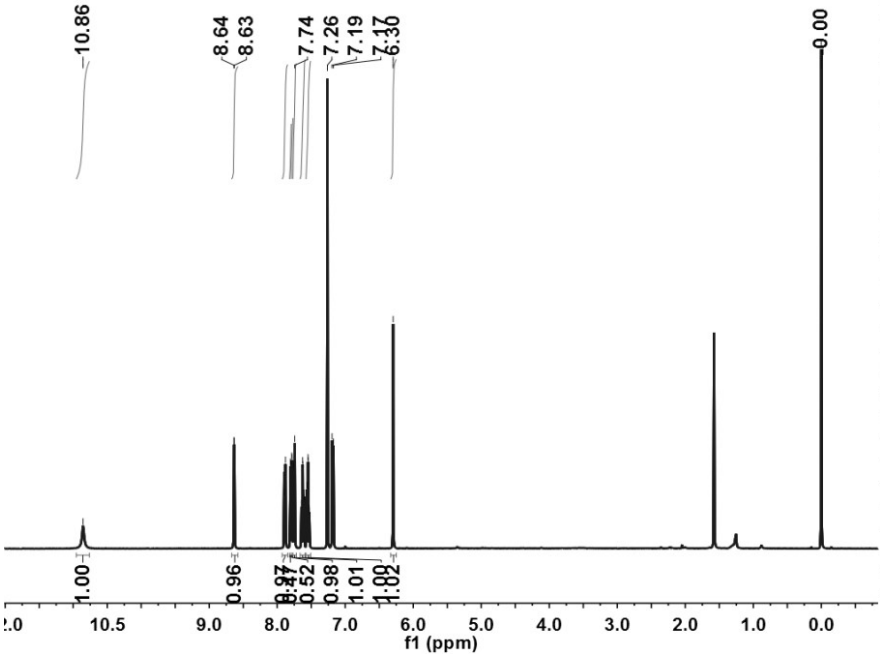

Figure S9. ^{1}H NMR spectrum of **1** in $CDCl_3$.

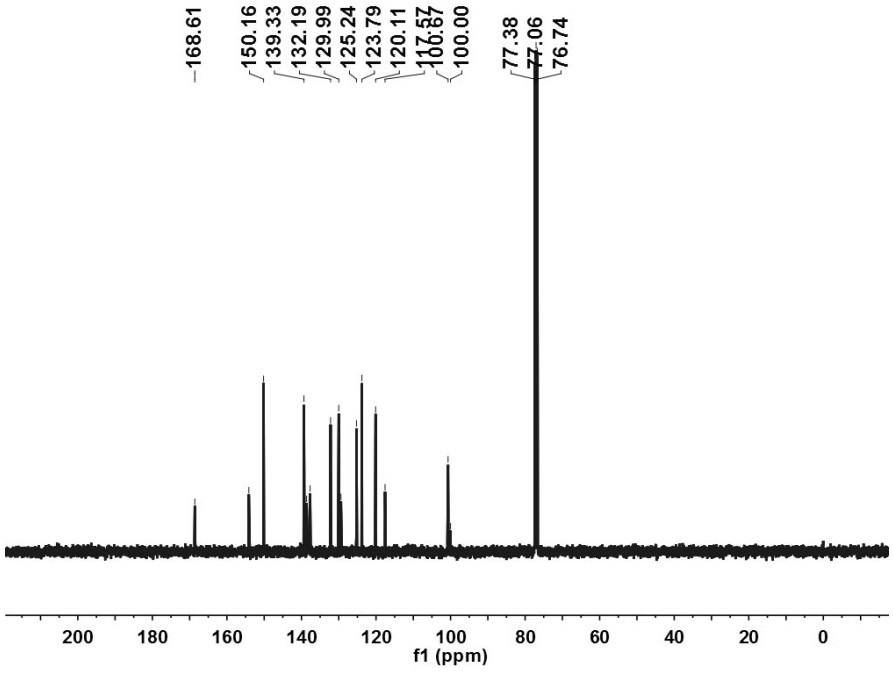

Figure S10. ^{13}C NMR spectrum of **1** in $CDCl_3$.

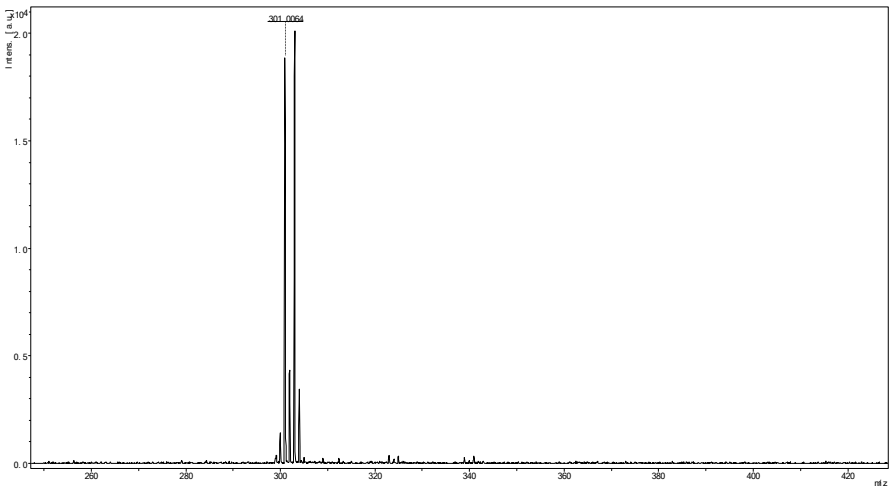

Figure S11. MALDI-TOF spectrum of **1**.

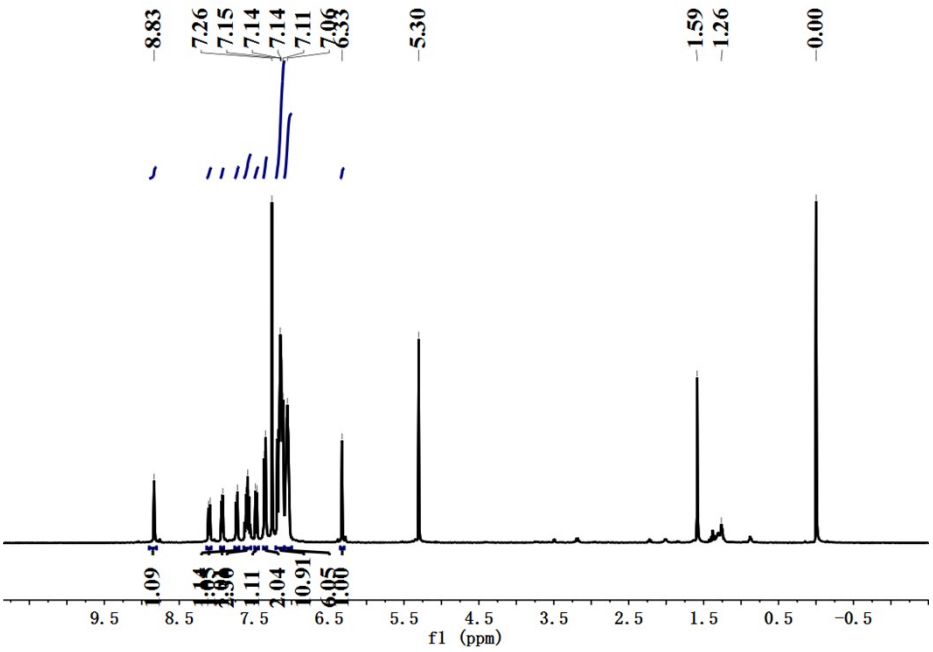

Figure S12. ^{1}H NMR spectrum of **2** in $CDCl_3$.

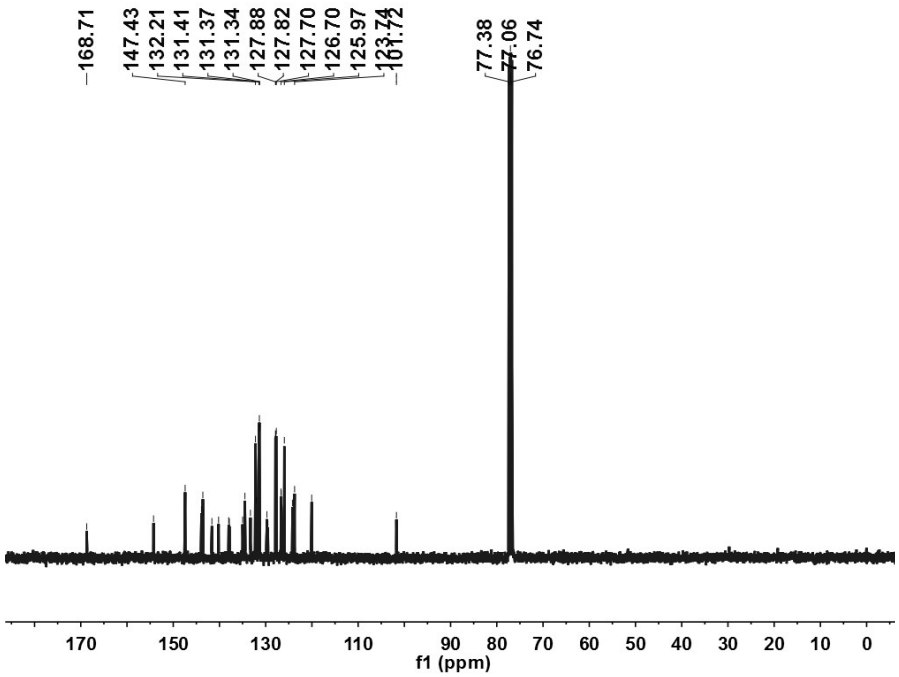

Figure S13. ^{13}C NMR spectrum of **2** in $CDCl_3$.

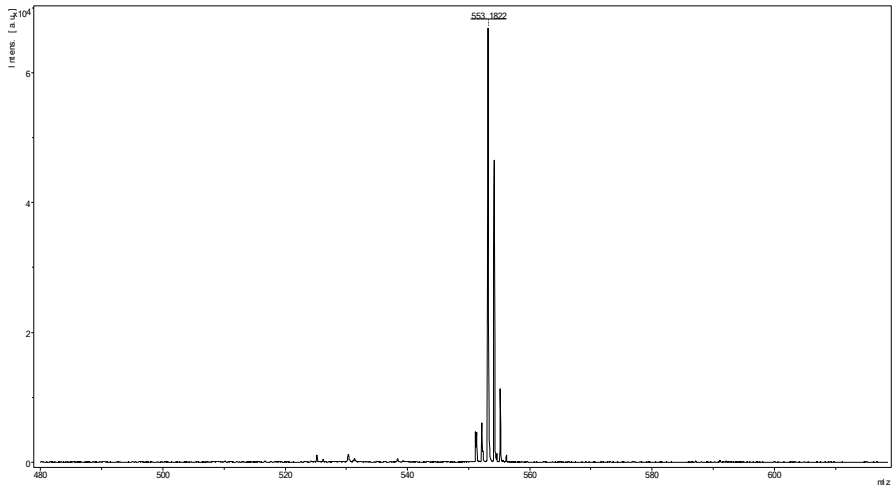

Figure S14. MALDI-TOF spectrum of **2**.

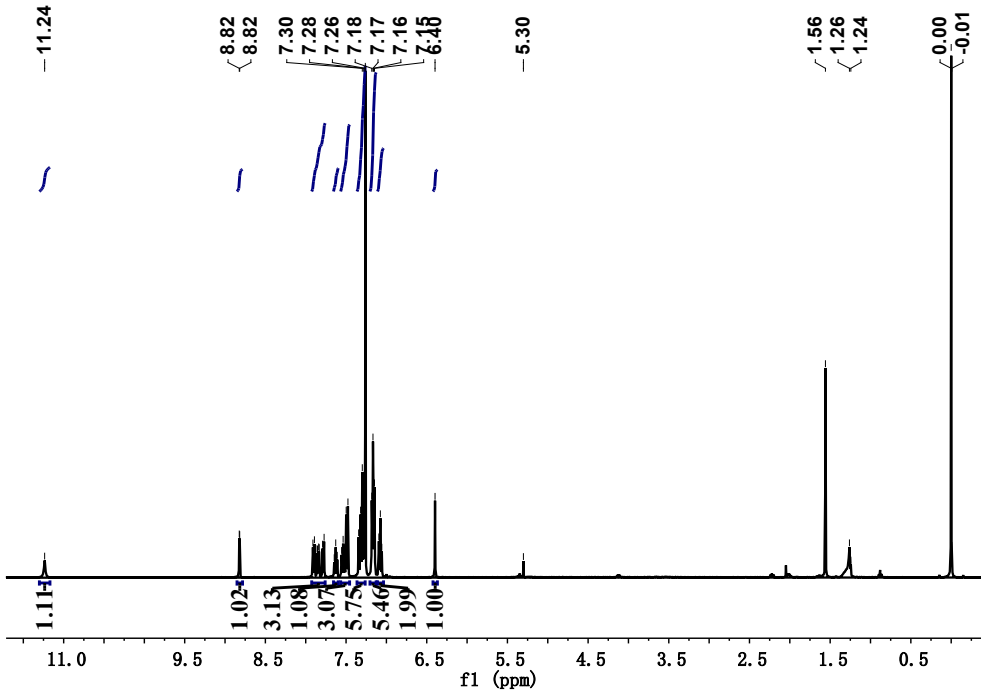

Figure S15. ^{1}H NMR spectrum of **3** in $CDCl_3$.

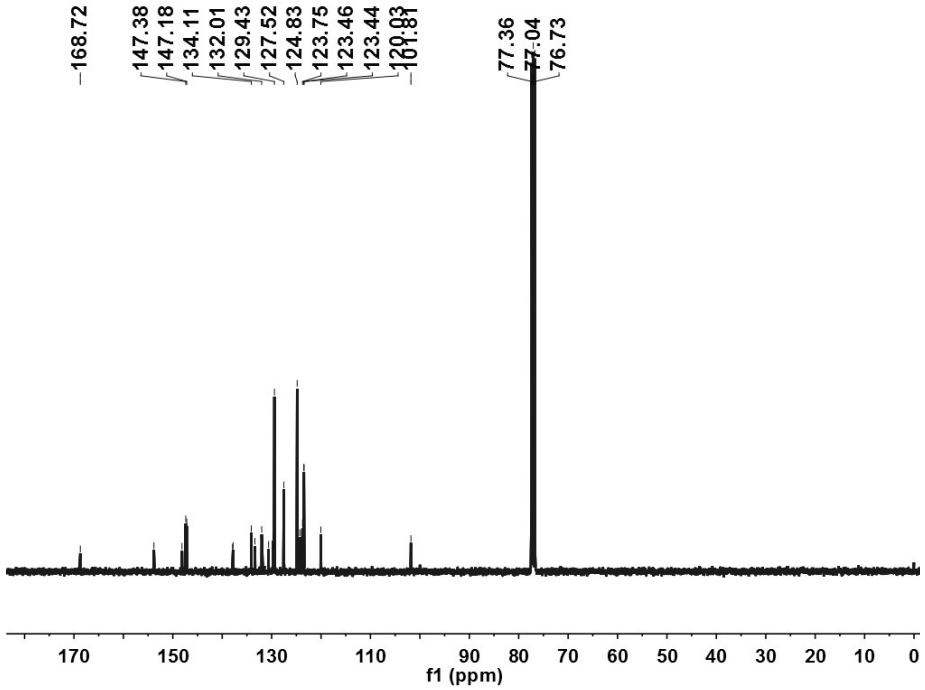

Figure S16. ^{13}C NMR spectrum of **3** in $CDCl_3$.

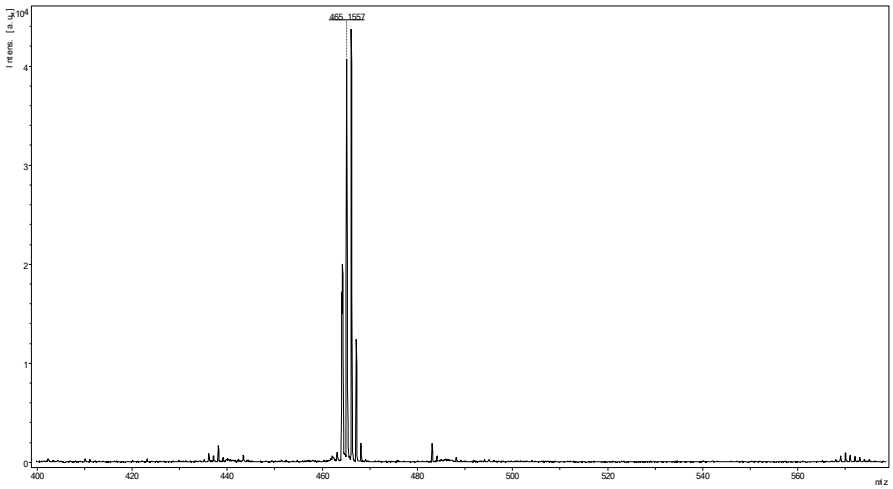

Figure S17. MALDI-TOF spectrum of **3**.

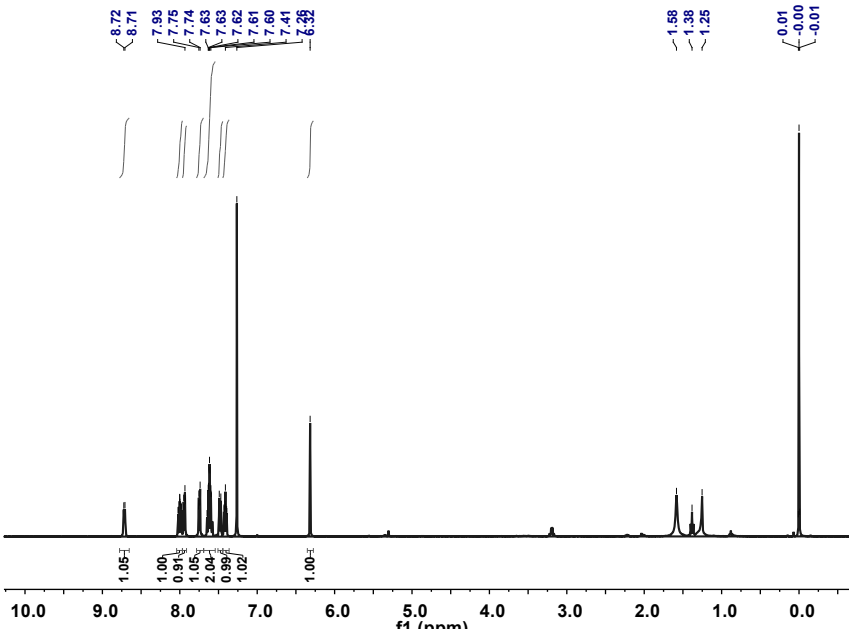

Figure S18. ^{1}H NMR spectrum of **B1** in $CDCl_3$.

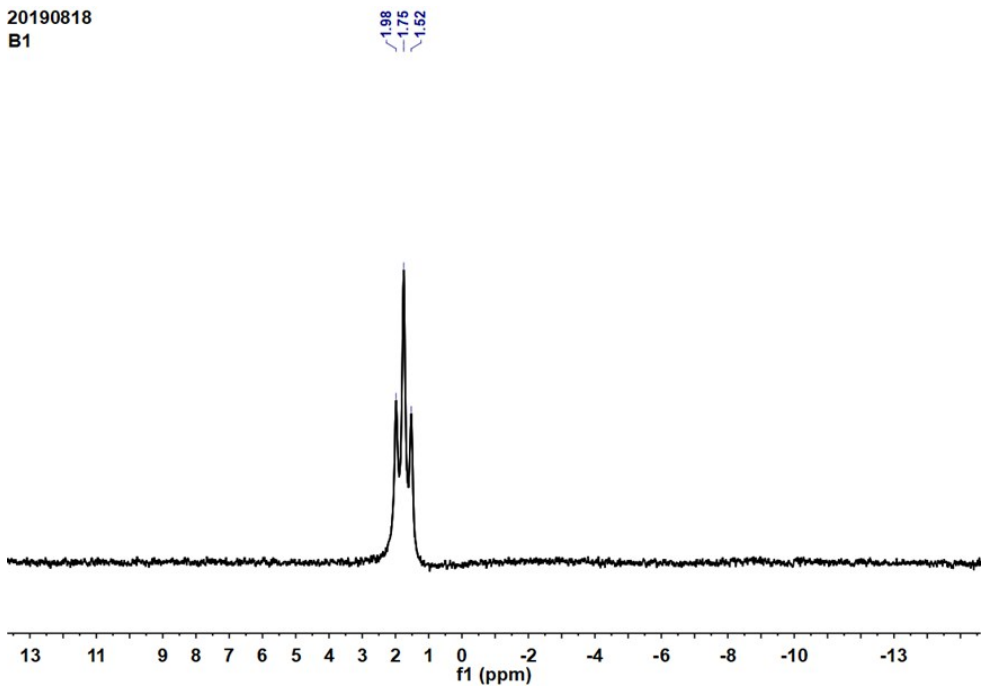

Figure S19. ^{11}B NMR spectrum of **B1** in $CDCl_3$.

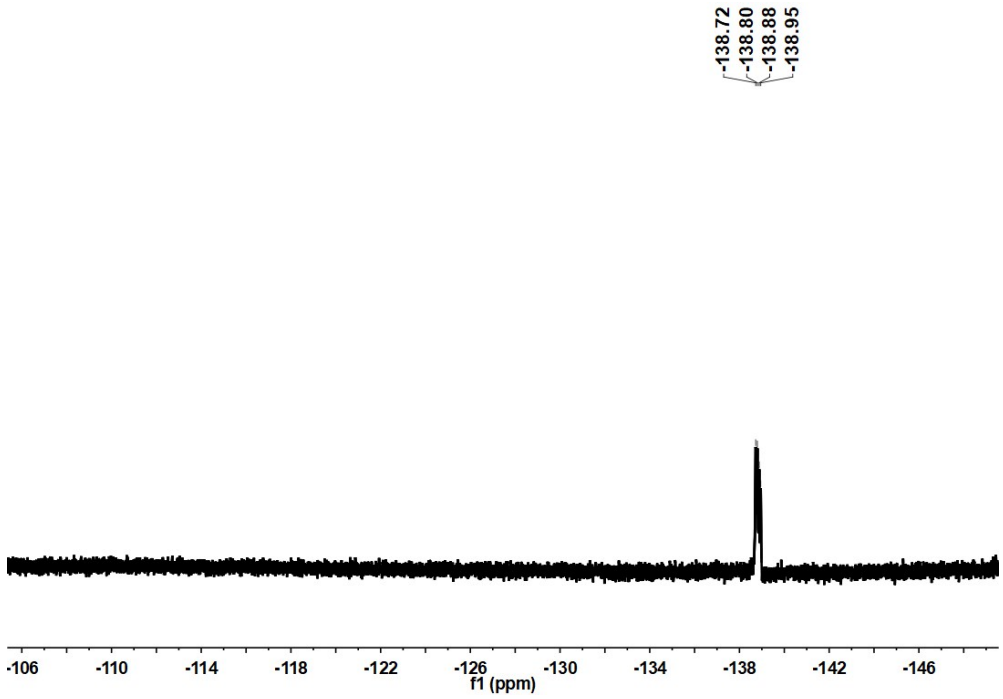

Figure S20. ^{19}F NMR spectrum of **B1** in $CDCl_3$.

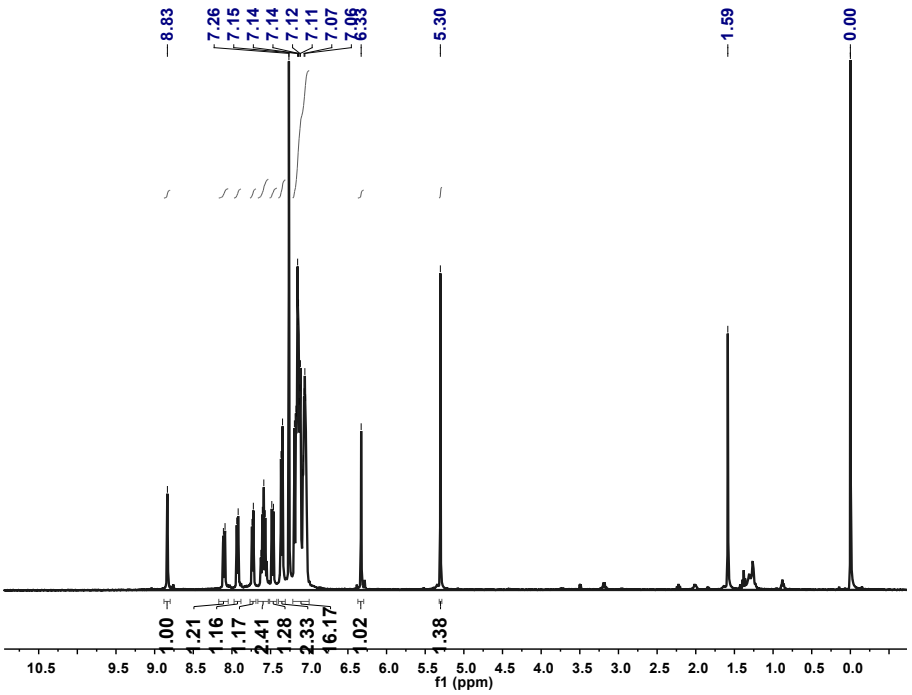

Figure S21. ^{1}H NMR spectrum of **B2** in $CDCl_3$.

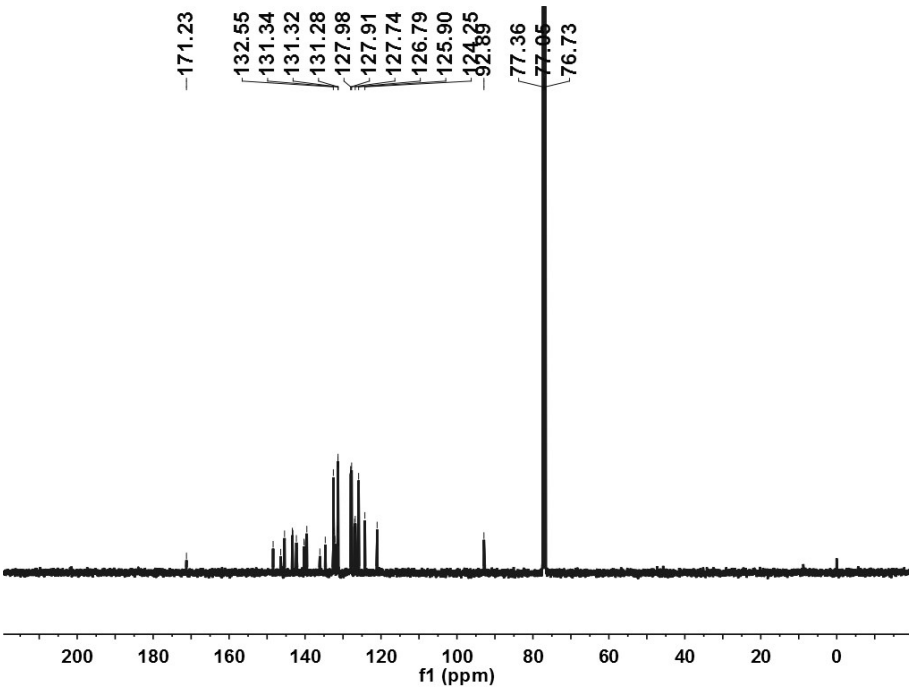

Figure S22. ^{13}C NMR spectrum of **B2** in $CDCl_3$.

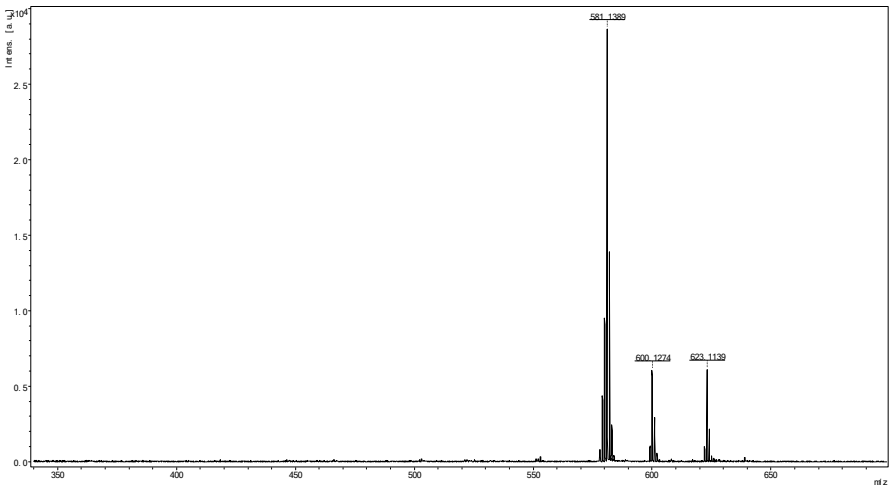

Figure S23 MALDI-TOF spectrum of **B2**

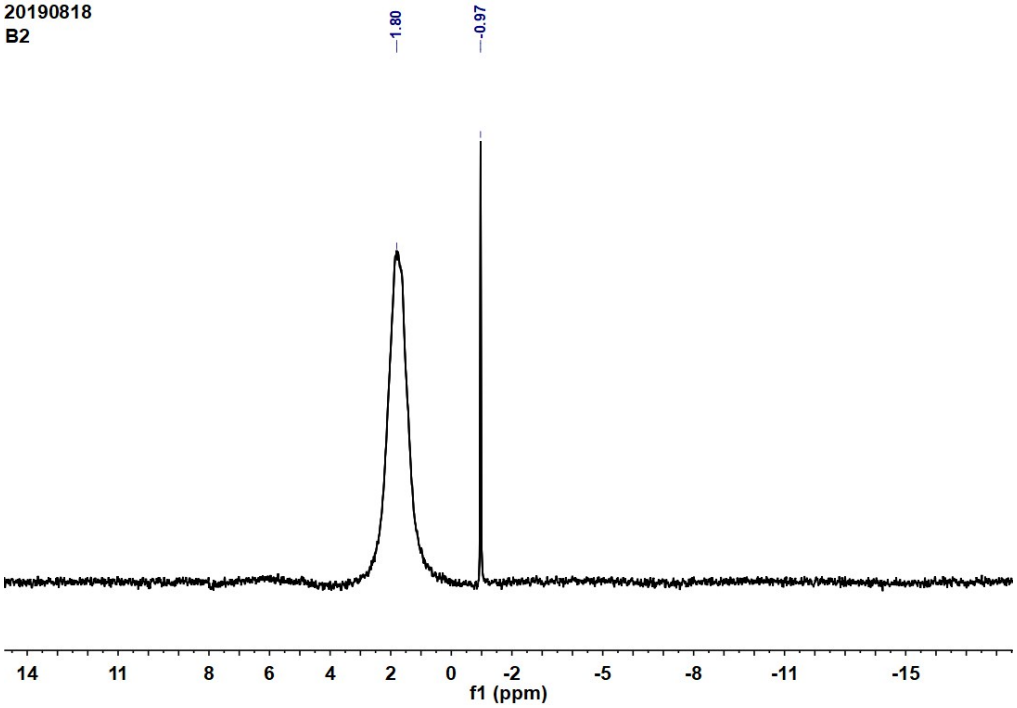

Figure S24. ^{11}B NMR spectrum of **B2** in $CDCl_3$.

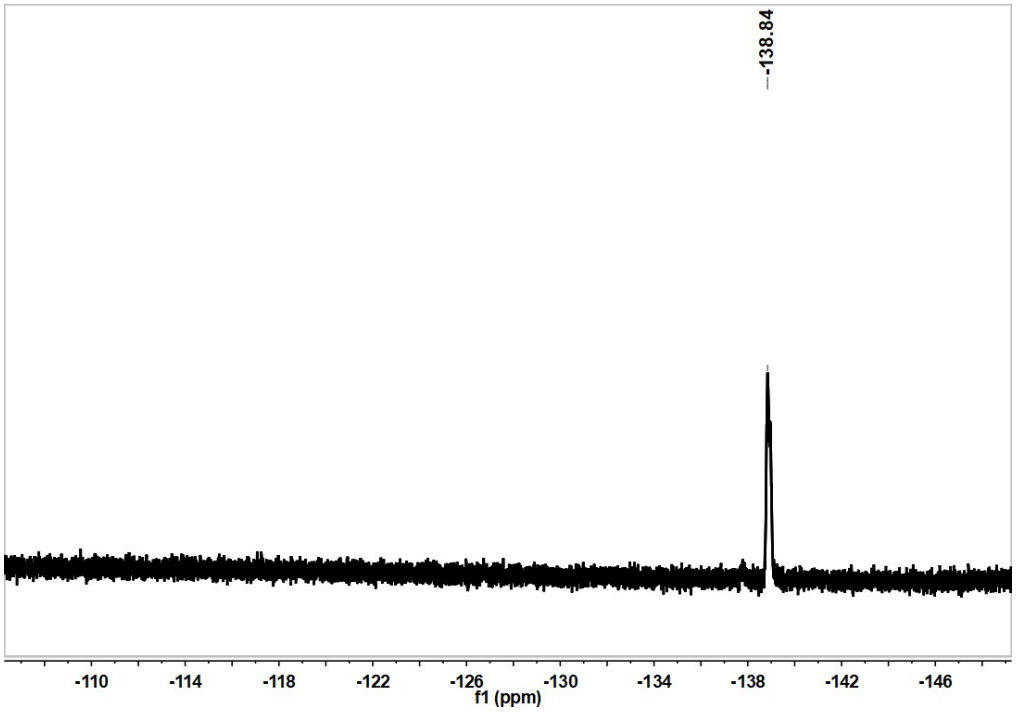

Figure S25. ^{19}F NMR spectrum of **B2** in $CDCl_3$.

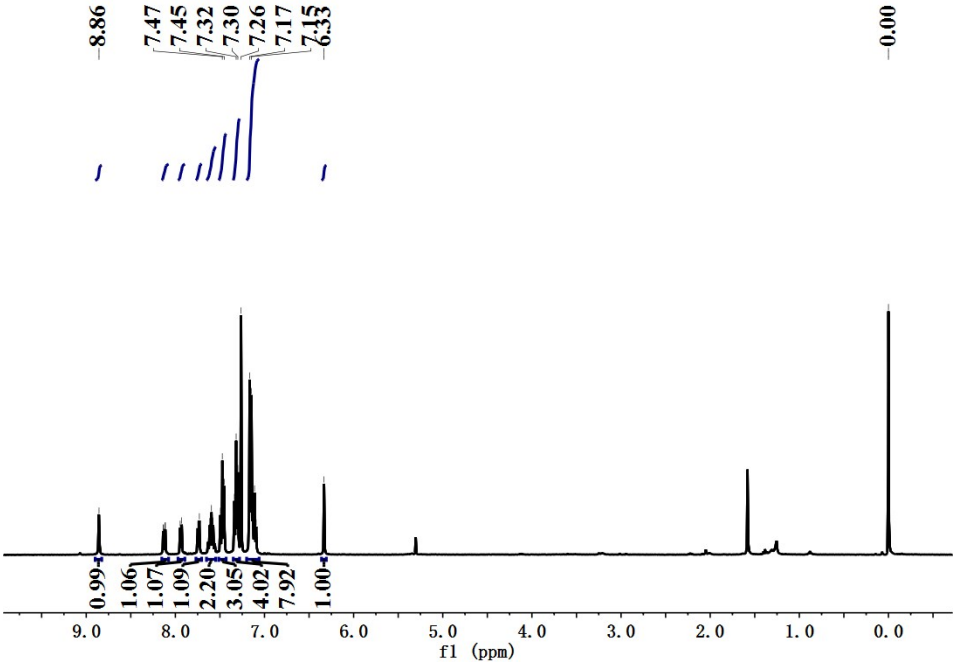

Figure S26. ^{1}H NMR spectrum of **B3** in $CDCl_3$.

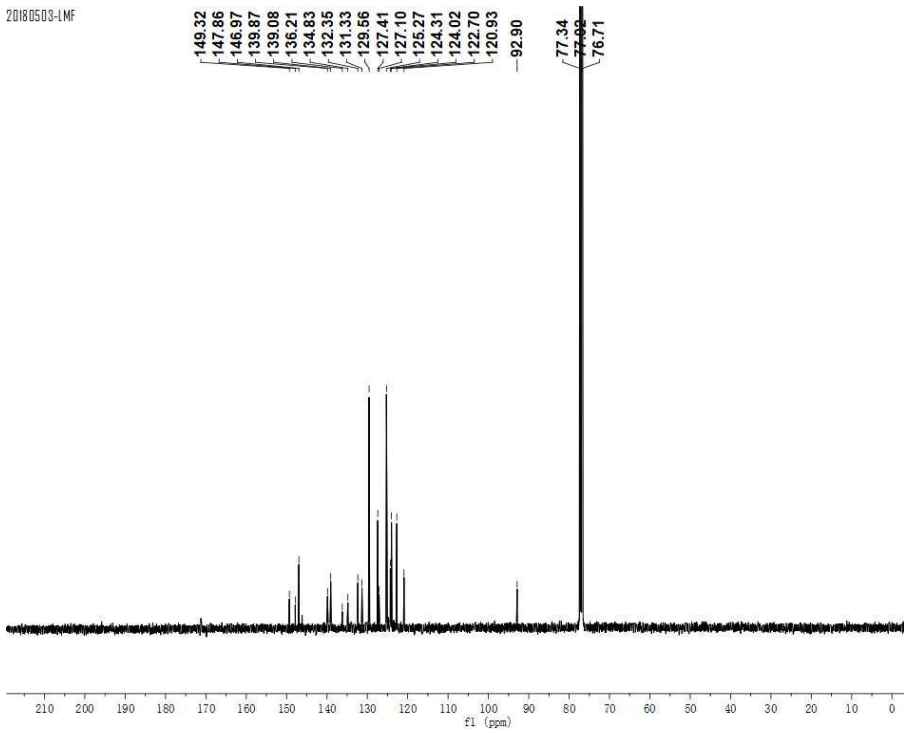

Figure S27. ^{13}C NMR spectrum of **B3** in $CDCl_3$.

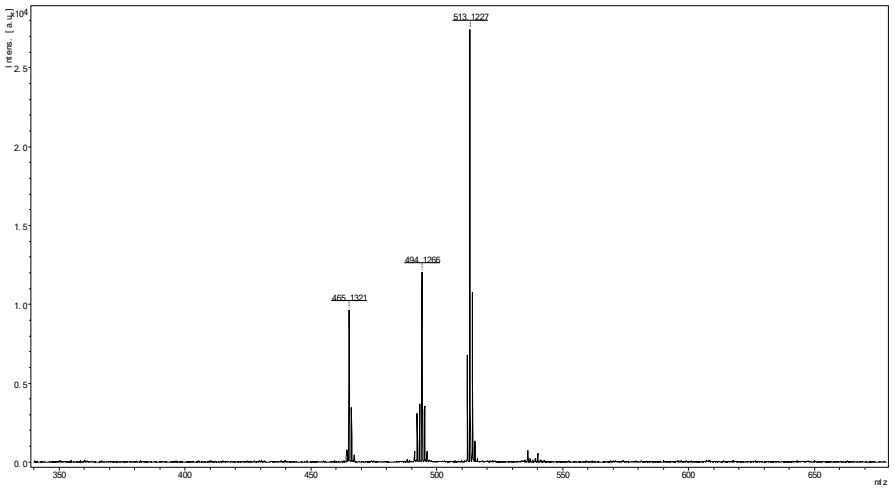

Figure S28. MALDI-TOF spectrum of **B3.**

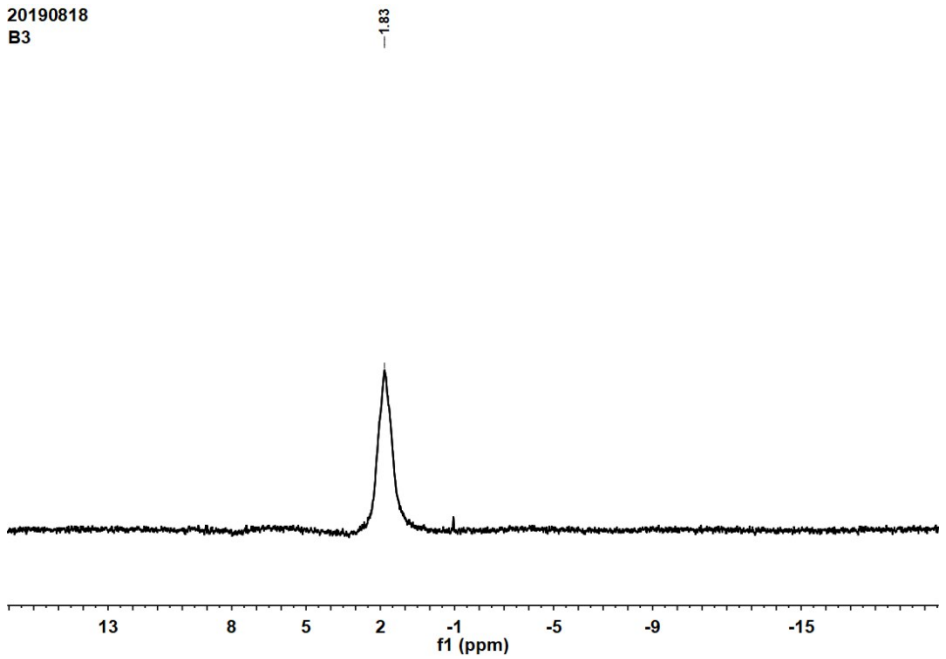

Figure S29. ^{11}B NMR spectrum of **B3** in $CDCl_3$.

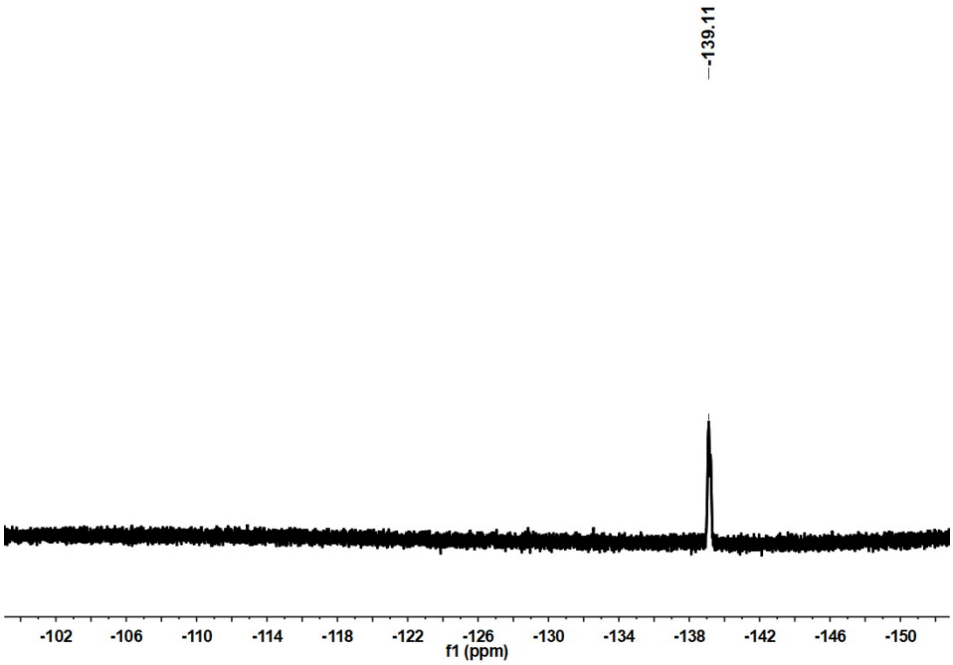

Figure S30. ^{19}F NMR spectrum of **B3** in $CDCl_3$.

6. References

S1. D. R. Coulson, *Inorg. Synth*. 1972, **13**, 121.

S2. Y. Zhou, Y. Xiao, D. Li, M. Y. Fu, X. H. Qian, *J. Org. Chem*. 2008, **73**, 1571.

S3. R. Misra, T. Jadhav, B. Dhokale, S. M. Mobina, *Chem. Comm.* 2014, **50**, 9076.

S4. J. Yang, Z. Ren, Z. Xie, Y. Liu, C. Wang, Y. Xie, Q. Peng, B. Xu, W. Tian, F. Zhang, Z. Chi, Q. Li, Z. Li, *Angew. Chem*. 2017, **129**, 898.